

Influence of Rare Earth Doping on the Structural and Catalytic Properties of Nanostructured Tin Oxide

Humberto V. Fajardo · Elson Longo · Luiz F. D. Probst · Antoninho Valentini ·
Neftalí L. V. Carreño · Michael R. Nunes · Adeilton P. Maciel ·
Edson R. Leite

Received: 3 March 2008 / Accepted: 7 May 2008 / Published online: 28 May 2008
© to the authors 2008

Abstract Nanoparticles of tin oxide, doped with Ce and Y, were prepared using the polymeric precursor method. The structural variations of the tin oxide nanoparticles were characterized by means of nitrogen physisorption, carbon dioxide chemisorption, X-ray diffraction, and X-ray photoelectron spectroscopy. The synthesized samples, undoped and doped with the rare earths, were used to promote the ethanol steam reforming reaction. The SnO_2 -based nanoparticles were shown to be active catalysts for the ethanol steam reforming. The surface properties, such as surface area, basicity/base strength distribution, and catalytic activity/selectivity, were influenced by the rare earth doping of SnO_2 and also by the annealing temperatures. Doping led to chemical and micro-structural variations at the surface of the SnO_2 particles. Changes in the catalytic

properties of the samples, such as selectivity toward ethylene, may be ascribed to different dopings and annealing temperatures.

Keywords Tin oxide · Rare earth · Nanocatalysts · Ethanol steam reforming · Basic sites

Introduction

The importance of the morphological properties of materials can be evidenced by the large number of publications on their synthesis. The development of new synthesis methods may lead to materials, such as catalysts, with superior performance. It is interesting to produce materials with nanometric-scale structures to obtain specific properties. Tin oxide nanoparticles have been investigated in our laboratory. This oxide has been used in a large range of technological applications, including sensors, catalysts, and electrocatalytic materials. It is well known that semiconductor oxides, such as SnO_2 , have an excellent potential for these applications due to their high capacity to adsorb gaseous molecules and promote their reactions [1–8]. We recently showed that the modification of the nanometric-scale structure and the composition of particles led to interesting selectivity changes for the methanol decomposition and aldolization reaction between acetone and methanol [2–4]. However, the influence of the nature of the active sites (the surface basicity of the oxide) on the performance of the catalysts was not totally investigated. The study of basicity, in more sensitive reactions, is very important as a source of information on the different kinds of active sites. In order to investigate the catalytic properties of the tin oxide samples prepared, we present the preliminary results in the catalytic steam reforming of

H. V. Fajardo (✉) · E. Longo
Instituto de Química de Araraquara, Departamento de
Bioquímica e Tecnologia Química, Universidade Estadual
Paulista, Rua Francisco Degni s/n, Quitandinha 14801-907
Araraquara, SP, Brasil
e-mail: hfajardoufsc@hotmail.com; hfajardo@qmc.ufsc.br

L. F. D. Probst
Departamento de Química, Universidade Federal de Santa
Catarina, 88040-900 Florianópolis, SC, Brasil

A. Valentini
Departamento de Química Analítica e Físico-Química,
Universidade Federal do Ceará, 60451-970 Fortaleza, CE, Brasil

N. L. V. Carreño · M. R. Nunes
Departamento de Química Analítica e Inorgânica, Universidade
Federal de Pelotas, 96010-900 Capão do Leão, RS, Brasil

A. P. Maciel · E. R. Leite
Departamento de Química, Universidade Federal de São Carlos,
13560-905 São Carlos, SP, Brasil

ethanol. This reaction is promoted not only by basic sites but also by acidic sites of the oxide catalysts. Thus, it may be suggested that the control of surfaces and modifications of the nanostructures of the tin oxide particles, undoped and doped with rare earths used as catalysts in this reaction, can be used to obtain additional information on the catalytic properties and application of these nanostructured materials. Nowadays, this process has gained increasing attention due to the possibility of obtaining hydrogen for fuel cell applications, as well as ethylene which is considered a valuable raw material in the polymeric industry [9–11].

Experimental

Sample Preparation

Doped and undoped SnO_2 samples were synthesized by the polymeric precursor method. This method is based on the chelation of cations (metals) by citric acid, in aqueous solution containing tin citrate, in the present case. Ethylene glycol was then added to polymerize the organic precursor. The aqueous tin citrate solution was prepared from $\text{SnCl}_2 \cdot \text{H}_2\text{O}$ (Mallinckrodt Baker, USA, purity >99.9%) and citric acid (Merck, Germany, purity >99.9%) with a citric acid:metal molar ratio of 3:1. For the synthesis of the rare earth-doped SnO_2 samples, an aqueous solution of a rare earth citrate was prepared from a rare earth nitrate (Y and Ce-nitrates, Alfa Aesar, USA, purity >99.9%) and citric acid with a citric acid:metal molar ratio of 3:1. The aqueous rare earth citrate solution was added to the aqueous tin citrate solution in the appropriate amount to obtain a doping level of 5 mol% in all cases. Ethylene glycol was then added to the citrate solutions, at a mass ratio of 40:60 in relation to citric acid, to promote the polymerization reaction. After several hours of polymerization at approximately 100 °C, the polymeric precursors were heat-treated in two steps, initially at 300 °C for 6 h in air to promote the pre-pyrolysis, and then at several temperatures (550–1,100 °C) for 2 h, also in air, to allow the organic material to be completely oxidized and to promote the crystallization of the SnO_2 phase.

Sample Characterization

The specific surface area of the samples was determined by N_2 adsorption/desorption isotherms (BET method) at liquid nitrogen temperature in an Quantachrome Autosorb-1C instrument. The CO_2 adsorption isotherms were determined with the same instrument. The amount of irreversible CO_2 uptake was obtained from the difference between the total adsorption of CO_2 on the catalyst and a second adsorption series of CO_2 determined after

evacuation of the catalyst sample for 20 min. X-ray diffraction (XRD; Siemens, D5000, equipped with graphite monochromator and Cu $K\alpha$ radiation) was used for the crystal phase determination. The X-ray photoelectron spectra were taken using a commercial VG ESCA 3000 system. The base pressure of the analysis chamber was in the low 10–10 mbar range. The spectra were collected using Mg $K\alpha$ radiation and the overall energy resolution was around 0.8 eV. The concentration of the surface elements was calculated using the system database after subtracting the background counts.

Catalyst Testing

Catalytic performance tests were conducted at atmospheric pressure with a quartz fixed-bed reactor (inner diameter 12 mm) fitted in a programmable oven, at a temperature of 500 °C. The catalysts (undoped SnO_2 sample calcined at 1,000 °C, Sn#1000, Y-doped SnO_2 samples calcined at 550 and 1,000 °C, SnY#550 and SnY#1000, respectively, and Ce-doped SnO_2 samples calcined at 550 and 1,000 °C, SnCe#550 and SnCe#1000, respectively) were previously treated in situ under nitrogen atmosphere at 500 °C for 2 h. The water:ethanol mixture (molar ratio 3:1) was pumped into a heated chamber and vaporized. The water–ethanol gas (N_2) stream (30 mL/min) was then fed to the reactor containing 150 mg of the catalyst. The reactants and the composition of the reactor effluent were analyzed with a gas chromatograph (Shimadzu GC 8A), equipped with a thermal conductivity detector (TCD), Porapak-Q, and a 5A molecular sieve column with Ar as the carrier gas. Reaction data were recorded for 4 h.

Results and Discussion

The characterization of undoped and rare earth-doped tin oxide nanoparticles has been previously reported [3]. Figure 1 illustrates the XRD patterns of the phase evolution of the undoped and doped (Ce and Y) SnO_2 particles annealed at different temperatures. Diffraction peaks related to a secondary phase formation ($\text{Sn}_2\text{Y}_2\text{O}_7$) for Y-doped SnO_2 were observed above a 900 °C heat-treating temperature. A secondary phase formation was also observed for Ce-doped SnO_2 samples; however, the CeO_2 phase was detected at an annealing temperature of 1,100 °C. On the other hand, for the samples annealed at temperatures lower than this, only the tetragonal SnO_2 phase was observed, suggesting the formation of a solid solution for the different dopants. The heat treatment promotes a segregation process, resulting in a surface with a different chemical composition. The X-ray diffraction patterns, associated with the Rietveld refinement method, were used to

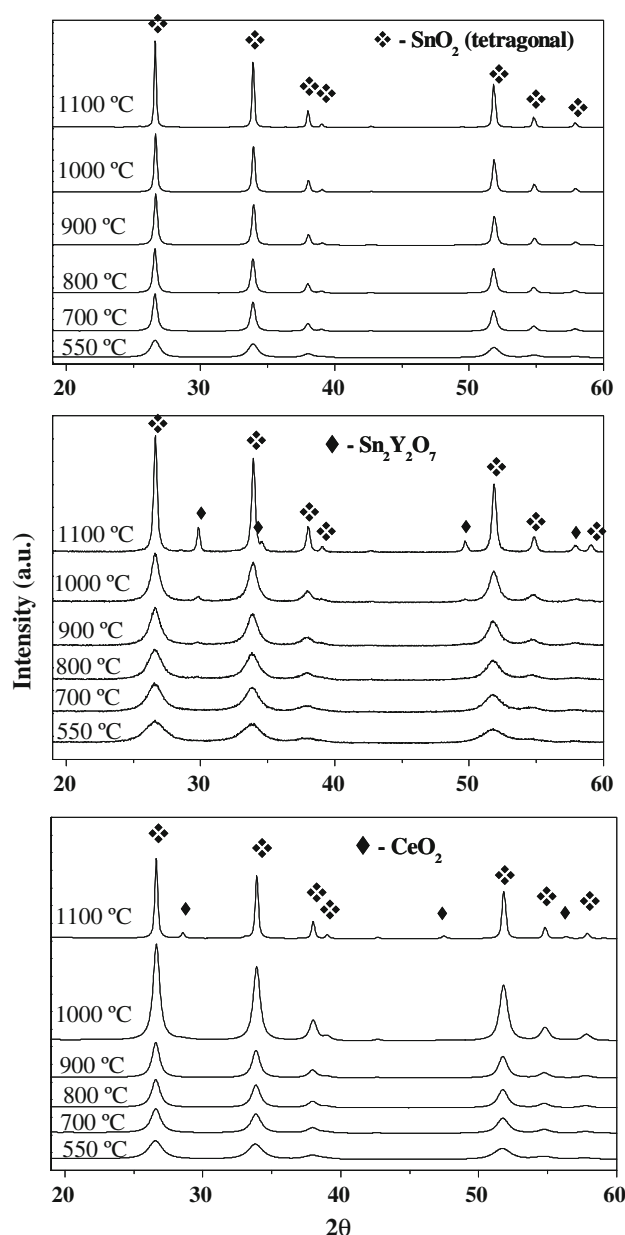


Fig. 1 X-ray diffraction results showing the phase evolution of the undoped SnO_2 , Ce- SnO_2 and Y- SnO_2 systems as a function of the heat-treatment temperature

determine the crystallite size of the tin oxide samples (Table 1), where it can be seen that the doping effect on the stability in terms of particle growth at high temperatures was remarkable. The results observed in the XRD analysis, secondary phase formations ($\text{Sn}_2\text{Y}_2\text{O}_7$ and CeO_2) depending on the annealing temperature, suggest that a de-mixing process occurs at higher temperatures. In order to obtain more information on this de-mixing process, X-ray photoemission spectroscopy (XPS) analysis was carried out. Figure 2a and b shows the X-ray photoemission spectroscopy results ([rare earth]/[Sn] ratio) for the Y- and

Table 1 Crystallite sizes measured by the Rietveld refinement and specific surface areas determined by N_2 adsorption (BET), as a function of the annealing temperature

Samples	Crystallite size (\AA)		Specific surface area (BET) ($\text{m}^2 \text{g}^{-1}$)	
	550 ^a	1,000 ^a	550 ^a	1,000 ^a
SnO_2	127.3	659.5	24	8
$\text{SnO}_2\text{-Y}$	52.2	143.4	63	17
$\text{SnO}_2\text{-Ce}$	117.2	194.5	48	16

^a Annealing temperature ($^\circ\text{C}$)

Ce-doped SnO_2 samples subjected to different thermal treatment temperatures. There is a general tendency for the concentration of Y on the surface of the samples to increase with an increase in annealing temperature. Both Y-doped samples, shown in Fig. 2a, present the 3d Y profile, indicating the presence of a secondary phase ($\text{Sn}_2\text{Y}_2\text{O}_7$), which

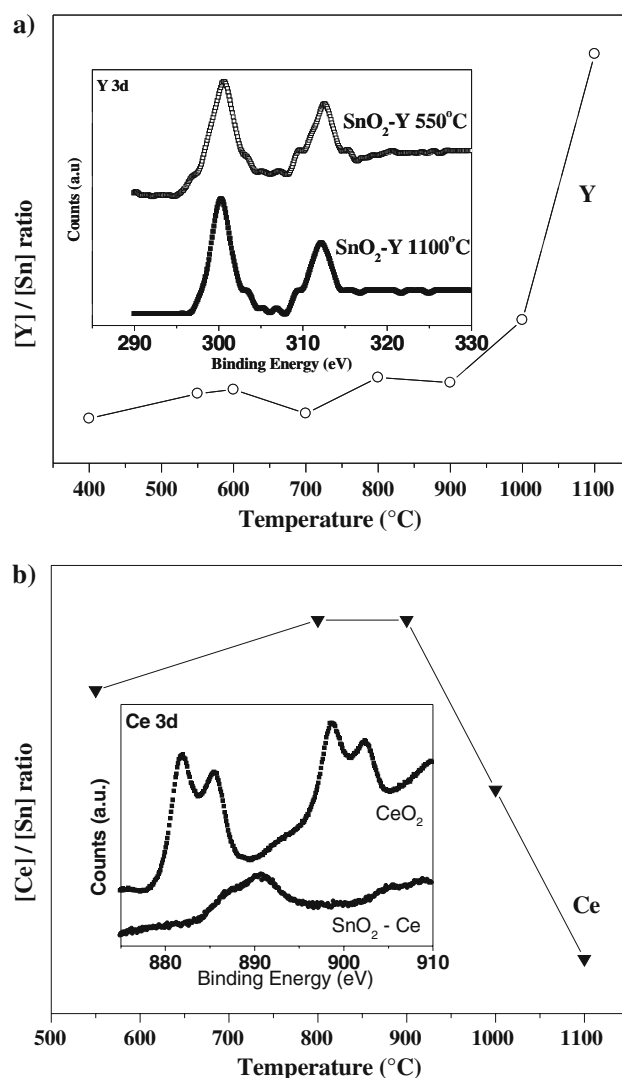
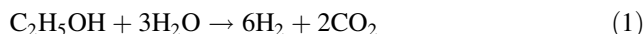


Fig. 2 The XPS results of [rare earth]:[Sn] ratio for Y- and Ce-doped SnO_2 samples subjected to different treatment temperatures

was detected in the XRD measurements. The results for the Ce-doped SnO_2 reveal a thermal behavior differing from that of the Y-doped samples. The $[\text{Ce}]/[\text{Sn}]$ concentration increases up to 900 °C, after which it decreases considerably as the annealing temperature rises. The inset shows the Ce 3d XPS lines (Fig. 2b). This behavior agrees with the shape of the Ce XPS pattern suggesting a non-homogenous covering of CeO_2 on the surface of the Ce- SnO_2 particles, in contrast to the homogenous covering of rare earth stannate observed in the Y-doped SnO_2 . It is clear, from the XPS results, that a surface rich in foreign cations is formed during the heat treatment. The de-mixing process observed for the Y-doped SnO_2 differs from that of Ce-doped SnO_2 . These results are in agreement with the XRD data and show the formation of stannate during heat treatments. As mentioned above, the heat treatment promotes a segregation process, resulting in a surface with different chemical compositions. For the Y-doped SnO_2

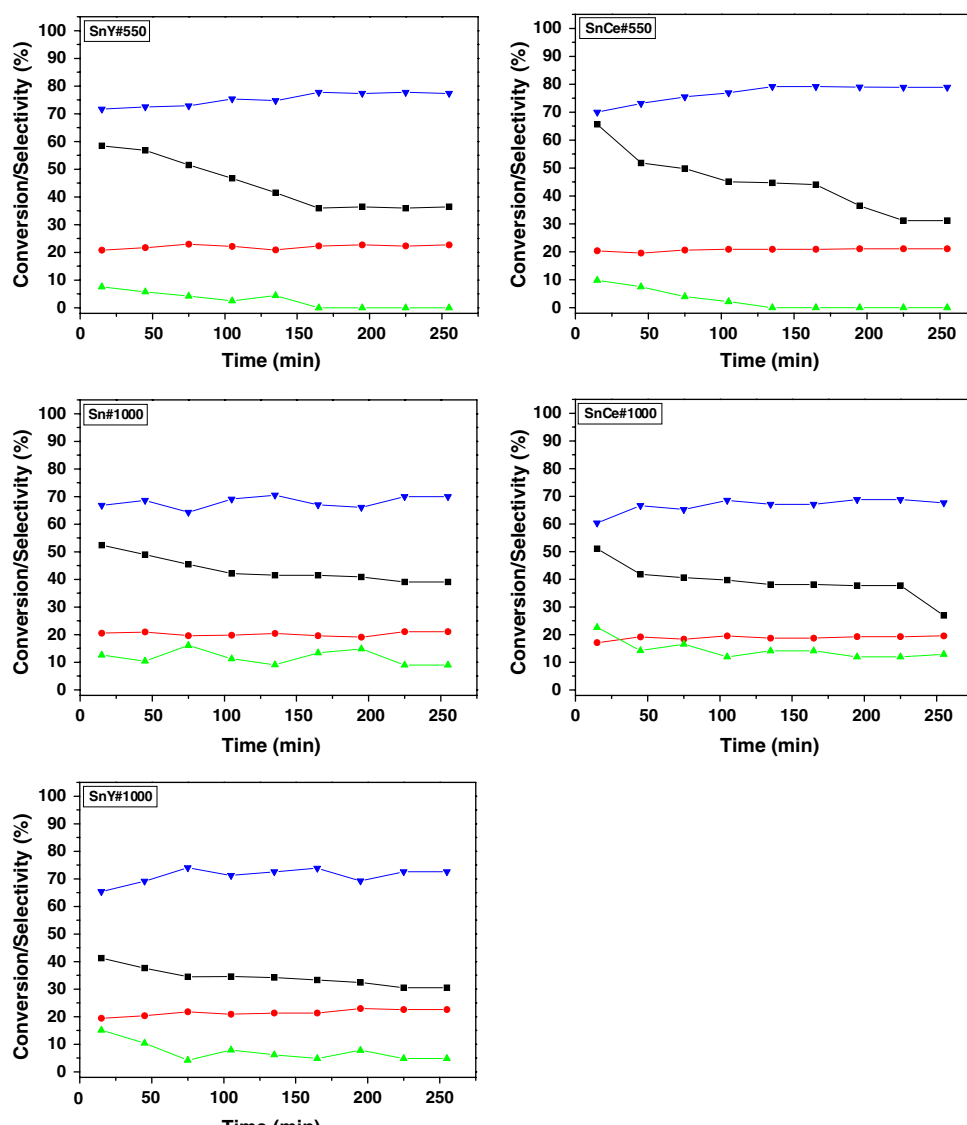
samples the ratio between $[\text{Y}]$ and $[\text{Sn}]$ increased with the heat treatment temperature, indicating that the dopant migrated toward the surface. On the other hand, the ratio between $[\text{Ce}]$ and $[\text{Sn}]$ decreased above 900 °C, suggesting that the dopant was expelled from the matrix [3].

In order to investigate the catalytic activity of the synthesized samples, the steam reforming of ethanol (Eq. 1) was carried out.

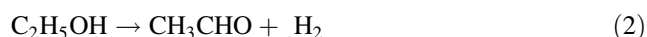


The effects of the process of segregation and de-mixing of these rare earths on the SnO_2 catalytic properties were studied and compared. In spite of the relatively low specific surface areas presented, the catalysts achieved significant ethanol conversion values at the beginning of the test. The conversion of ethanol for the SnCe#550 catalyst was higher than for the Sn#1000 catalyst, indicating the positive effect of rare earth doping. From the results in Fig. 3, it can be seen that

Fig. 3 Catalytic performances of undoped and Y- and Ce-doped SnO_2 samples in the steam reforming of ethanol. Legends: ■ = $\text{C}_2\text{H}_5\text{OH}$ conversion; ● = H_2 ; ▲ = C_2H_4 ; ▼ = CH_3CHO selectivity, respectively



hydrogen, ethylene and acetaldehyde were the only products detected during the ethanol steam reforming process. However, it is interesting to observe that the catalysts presented a distinct behavior in terms of product selectivity. Acetaldehyde was the major product formed, with lower amounts of hydrogen and ethylene, indicating that ethanol dehydrogenation and dehydration reactions (Eqs. 2 and 3, respectively) are promoted over the catalyst surfaces.



According to the results, it can be seen that dehydration and dehydrogenation reactions are promoted over the undoped SnO_2 catalyst. SnO_2 is known as an amphoteric oxide, with a slightly acid character; thus, a combination of catalytic properties could be observed on the surface of this catalyst, indicating that this particular catalyst has a great ability for dehydration and dehydrogenation of ethanol. Nevertheless, the decrease in the production of ethylene over time, observed for the doped samples, may be indicative of a moderate modification of the material surface due to the doping with rare earths. One of the most common ways to modify the characteristics of a material is by introducing dopants. When introduced into a powder, they may follow different paths: diffuse into the bulk of the particle, form a new crystallographic structure or a solid solution, migrate to the surface (surface additives), or nucleate a second phase. Previous studies have evaluated the effect of different dopants on the morphology and properties of tin oxide. Rare earth cations have, as yet, been little explored as tin oxide dopants for catalytic purposes. However, the consensus is that their influence on the catalytic properties of SnO_2 is associated with the acid/base characteristics of the oxides involved. The surface modifications, due to doping process, change some macroscopic properties of the tin oxide, such as the isoelectric point. The isoelectric point of the pure SnO_2 can be shifted to basic pH values due to the introduction of a basic surface oxide in the SnO_2 matrix. Thus, the basic characteristics of rare earth oxides may favor some catalytic aspects such as the

presence of adsorbing centers [6, 12–15]. The reactions over $\text{SnCe}\#550$ and $\text{SnY}\#550$ start with H_2 , C_2H_4 , and CH_3CHO as the main products; however, the selectivity toward C_2H_4 decreases with a concomitant CH_3CHO production as the reaction progresses. The Y-doped SnO_2 sample annealed at 1,000 °C showed a similar catalytic behavior, in terms of product selectivities, comparatively to the Ce- and Y-doped SnO_2 samples annealed at 550 °C. On the other hand, the $\text{SnCe}\#1000$ catalyst presented a distinct behavior, displaying a higher value of selectivity toward C_2H_4 . The reaction pathway during catalytic ethanol steam reforming comprises a series of simultaneous reactions. These reactions are more or less promoted depending on the nature of the catalyst, the type of interaction with the surface of the solid material, and the different reaction conditions [9, 10]. Ethanol is rapidly dehydrated and dehydrogenated over the catalysts under study. Ethylene and acetaldehyde seem to be primary products formed in the ethanol steam reforming, and the selectivity of this reaction can be influenced by the acidic–basic properties on the catalyst surface. Ethanol dehydration into ethylene is essentially catalyzed by the acidic sites while basic sites are predominant in the ethanol dehydrogenation into acetaldehyde. In addition, the strength of the acidic and basic sites is a determining factor in the reaction kinetics [9, 10]. With the aim of obtaining more information on the surface properties of the catalysts prepared, CO_2 adsorption analysis was carried out. Carbon dioxide was the probe molecule used to determine the basic properties of the catalysts. The results from the isotherms of the CO_2 adsorption are shown in Table 2. The CO_2 adsorption isotherms are very sensitive to the presence of polar groups or ions on the surface of the solid [16]. It was evident that the CO_2 adsorption capacity of undoped SnO_2 samples can be significantly affected by the doping chemical species and by the annealing treatment. In the samples treated at 550 °C, it was observed that the total amount of CO_2 adsorbed (at 27 °C) for the Y-doped SnO_2 sample was around six times higher than that of the undoped sample. It is observed that the increase in the annealing temperature

Table 2 The total and irreversible CO_2 adsorption capacity, uptake at 27 and 300 °C, of undoped and doped samples of tin oxide

Samples	Total CO_2 adsorption ($\mu\text{mol}/\text{m}^2$)				Irreversible CO_2 adsorption ($\mu\text{mol}/\text{m}^2$)			
	550 ^a		1,000 ^a		550 ^a		1,000 ^a	
	27 ^b	300 ^b	27 ^b	300 ^b	27 ^b	300 ^b	27 ^b	300 ^b
SnO_2	0.54	0.34	0.81	0.93	0.20	–	0.13	0.16
$\text{SnO}_2\text{-Ce}$	1.66	0.61	2.05	1.48	0.76	0.12	0.45	–
$\text{SnO}_2\text{-Y}$	3.23	0.94	1.92	1.08	1.32	0.12	1.04	0.18

^a Annealing temperature (°C)

^b Isotherm temperature adsorption (°C)

leads to significant changes in the basic sites in SnO_2 . It is important to point out the irreversible CO_2 adsorption uptake at 300 °C for the undoped and Y-doped SnO_2 samples. These results suggest that a higher annealing temperature promotes an increase in the stronger basic sites. On the other hand, for the Ce-doped SnO_2 sample treated at 1,000 °C, the isotherms taken at 300 °C did not present an irreversible CO_2 adsorption. Therefore, a basic oxide, such as yttrium oxide, introduced in the SnO_2 matrix promotes the basicity of the surface. The lower ethylene selectivity observed on the doped catalysts ($\text{SnCe}\#550$ and $\text{SnY}\#550$) is in agreement with the increase in surface basicity detected in the CO_2 adsorption analysis, with respect to the undoped SnO_2 . With the rare earth doping and the increase in the annealing temperature of the SnO_2 samples to 1,000 °C, another catalytic behavior was observed, probably as a result of the modification of the nanostructure and the basic sites of the particles. Another phenomenon starts to occur on the surface of doped samples, a segregation process of particles of metastable solid solution, promoted by the increase in the annealing temperature that may be related to the change in the catalytic behavior. The $\text{SnY}\#1000$ catalyst showed low selectivity toward ethylene. The $\text{SnCe}\#1000$ catalyst presented a higher value for ethylene selectivity. This may be associated with the high amount of secondary phases ($\text{Sn}_2\text{Y}_2\text{O}_7$ and CeO_2 , respectively) which are formed on the surface of SnO_2 samples, as the annealing temperature increases. The Y-doped sample annealed at 1,000 °C exhibited a dopant-rich surface, with the formation of $\text{Sn}_2\text{Y}_2\text{O}_7$, as shown above. As the annealing temperature increased, a surface area reduction took place, and the formation of a segregation layer increased the external foreign cation concentration and the stronger basic sites on the surface of the Y-doped samples. This may be directly associated with the specific characteristics of the catalytic process observed in these SnO_2 samples. Such behavior was not observed for the catalytic activity of the Ce-doped sample annealed at 1,000 °C. The CeO_2 de-mixing process did not seem to interfere with its catalytic properties, probably because CeO_2 , which is segregated on the SnO_2 surface, is a known catalyst with redox properties used to promote oxidation reactions.

Conclusions

The SnO_2 -based nanoparticles were shown to be active catalysts for the ethanol steam reforming reaction. The surface properties, such as surface area, basicity/base

strength distribution, and catalytic activity/selectivity, were influenced by the rare earth doping of SnO_2 and also by the annealing temperatures. Doping led to chemical and microstructural variations at the surface of the SnO_2 particles. Also, changes in the catalytic properties of the samples, such as selectivity toward ethylene, may be ascribed to different dopings and annealing temperatures. This suggests a new pathway to produce catalysts by means of controlling their surface. A super-saturated solid solution yields a nanostructured metastable material that will undergo foreign cation segregation to the outer surface and then a de-mixing process. This process can effectively be used to control the surface chemistry.

In the present study, the effect of the different operational conditions, such as reaction temperature and water:ethanol molar ratio, on the catalytic behavior was not determined. However, this study is under way, and it will be the subject of future reports.

Acknowledgments The authors gratefully acknowledge CNPq, FAPERGS, and FINEP for financial support.

References

1. I.T. Weber, A.P. Maciel, P.N. Lisboa-Filho, C.O. Paiva-Santos, W.H. Schreider, Y. Maniette, E.R. Leite, E. Longo, *Nanoletters* **2**, 969 (2002)
2. I.T. Weber, A. Valentini, L.F.D. Probst, E. Longo, E.R. Leite, *Sens. Actuators B* **97**, 31 (2004)
3. N.L.V. Carreño, A.P. Maciel, E.R. Leite, P.N. Lisboa-Filho, E. Longo, A. Valentini, L.F.D. Probst, C.O. Paiva-Santos, W.H. Schreiner, *Sens. Actuators B* **86**, 185 (2002)
4. N.L.V. Carreño, H.V. Fajardo, A.P. Maciel, A. Valentini, F.M. Pontes, L.F.D. Probst, E.R. Leite, E. Longo, *J. Mol. Catal. A* **207**, 89 (2004)
5. J. Zhang, L. Gao, *J. Solids State Chem.* **177**, 1425 (2004)
6. T. Jinkawa, G. Sakai, J. Tamaki, N. Miura, N. Yamazoe, *J. Mol. Catal. A* **155**, 193 (2000)
7. S. Ardizzone, G. Cappelletti, M. Ionita, A. Minguzzi, S. Rondini, A. Vertova, *Electrochim. Acta* **50**, 4419 (2005)
8. C.P. De Pauli, S. Trasatti, *J. Electroanal. Chem.* **145**, 538 (2002)
9. P.D. Vaidya, A.E. Rodrigues, *Chem. Eng. J.* **117**, 39 (2006)
10. A. Haryanto, S. Fernando, N. Murali, S. Adhikari, *Energy Fuels* **19**, 2098 (2005)
11. X. Li, B. Shen, Q. Guo, J. Gao, *Catal. Today* **125**, 270 (2007)
12. E.R. Leite, I.T. Weber, E. Longo, J.A. Varela, *Adv. Mater.* **12**, 965 (2000)
13. F. Lu, Y. Liu, M. Dong, X. Wang, *Sens. Actuators B* **66**, 225 (2000)
14. P.G. Harrison, C. Bailey, W. Azelee, *J. Catal.* **186**, 147 (1999)
15. G.J. Pereira, R.H.R. Castro, P. Hidalgo, D. Gouvêa, *Appl. Surf. Sci.* **195**, 277 (2002)
16. N.O. Lemcoff, K.S.W. Sing, *J. Colloid Interf. Sci.* **61**, 227 (1977)